ARTICLE

BIOTECHNOLOGY and BIOENGINEERING

Motility Analysis of Bacteria-Based Microrobot (Bacteriobot) Using Chemical Gradient Microchamber

Daechul Park,[1] Sung Jun Park,[1] Sunghoon Cho,[1] Yeonkyung Lee,[1] Yu Kyung Lee,[1] Jung-Joon Min,[2] Bang Ju Park,[3] Seong Young Ko,[1] Jong-Oh Park,[1] Sukho Park[1]

[1]School of Mechanical Systems Engineering, Chonnam National University, Gwangju 500-757, Korea; telephone: +82-62-530-1687; fax: +82-62-530-0267; e-mail: jop@jnu.ac.kr

[2]Department of Nuclear Medicine, Chonnam National University Medical School, Gwangju, Korea

[3]College of BioNano Technology, Gachon University, Gyeonggi-do, Korea

ABSTRACT: A bacteria-based microrobot (bacteriobot) was proposed and investigated as a new type of active drug delivery system because of its useful advantages, such as active tumor targeting, bacteria-mediated tumor diagnosis, and therapy. In this study, we fabricated a bacteriobot with enhanced motility by selective attachment of flagellar bacteria (*Salmonella typhimurium*). Through selective bovine serum albumin (BSA) pattering on hydrophobic polystyrene (PS) microbeads, many *S. typhimurium* could be selectively attached only on the unpatterned surface of PS microbead. For the evaluation of the chemotactic motility of the bacteriobot, we developed a microfluidic chamber which can generate a stable concentration gradient of bacterial chemotactic chemicals. Prior to the evaluation of the bacteriobot, we first evaluated the directional chemotactic motility of *S. typhimurium* using the proposed microfluidic chamber, which contained a bacterial chemo-attractant (L-aspartic acid) and a chemo-repellent ($NiSO_4$), respectively. Compared to density of the control group in the microfluidic chamber without any chemical gradient, *S. typhimurium* increased by about 16% in the L-aspartic acid gradient region and decreased by about 22% in the $NiSO_4$ gradient region. Second, we evaluated the bacteriobot's directional motility by using this microfluidic chamber. The chemotactic directional motility of the bacteriobot increased by 14% and decreased by 13% in the concentration gradients of L-aspartic acid and $NiSO_4$, respectively. These results confirm that the bacteriobot with selectively patterned *S. typhimurium* shows chemotaxis motility very similar to that of *S. typhimurium*. Moreover, the directional motilities of the bacteria and bacteriobot could be demonstrated quantitatively through the proposed microfluidic chamber.

Biotechnol. Bioeng. 2014;111: 134–143.

KEYWORDS: *Salmonella typhimurium*; microrobot; bacteriobot; microchamber; chemotaxis

Introduction

Recently, many researchers have used flagellar bacteria, such as *Escherichia coli*, *Salmonella typhimurium*, and *Serratia marcescens*, to most efficiently translocate a small but powerful niche force because of their strong merits such as movement or taxis (Berg, 2003; Bren and Eisenbach, 2000). Some researchers have reported anaerobic bacteria such as *Clostridia* and *Bifidobacteria* and facultative anaerobic bacteria such as *E. coli* or *Salmonella* are chemo-attracted by substances in quiescent or necrotic tumor cells (Kasinskas and Forbes, 2006). Moreover, when the chemotaxis of bacteria is controlled for particular tumor microenvironments, bacteria can be attracted to specific regions of solid tumors by some receptors (Leschner et al., 2009). Therefore, the chemotactic sensibility of bacteria has been studied as an important characteristic for biomedical applications (Eisenbach, 1996; Wadhams and Armitage, 2004).

Based on these properties of bacteria, a bacteria-based microrobot (bacteriobot), mainly consisting of a microstructure that represents the therapeutic drug body and the bacteria that act as the actuators and sensors of the microrobot, was proposed as a new type of active drug delivery system (Yoo et al., 2011). A prototype of the bacteriobot was developed as a combination of a polystyrene (PS) microbead and flagellar bacteria, which can attach to the surface of a hydrophobic PS microbead (Behkam and Sitti, 2008; Eldowney and Fletcher, 1986). In addition, the bacteria could be selectively patterned onto the microstructure to enhance the motility of the

Daechul Park and Sung Jun Park contributed equally to this work.

Correspondence to: J.-O. Park and S. Park

Contract grant sponsor: Future Pioneer R&D program through the National Research Foundation of Korea

Contract grant sponsor: Ministry of Education, Science, and Technology

Contract grant number: 2012-0001035

Received 26 February 2013; Revision received 8 July 2013; Accepted 15 July 2013

Accepted manuscript online 24 July 2013;

Article first published online 21 August 2013 in Wiley Online Library (http://onlinelibrary.wiley.com/doi/10.1002/bit.25007/abstract).

DOI 10.1002/bit.25007

bacteriobot (Behkam and Sitti, 2008; Cho et al., 2012; Park et al., 2010). For selective bacterial patterning onto the microstructure, we used several selective bacteria patterning methods. First, the flagellar bacteria *S. marcescens* were selectively attached to SU-8 microstructures by bovine serum albumin (BSA) selective patterning (Park et al., 2010). Second, we modified the selective surfaces of poly-ethylene-glycol (PEG) microbeads using poly-L-lysine (PLL) and modified the submerging property of PEG microbeads on agarose gel. By this process, *S. typhimurium* on could be patterned onto the PEG microbeads (Cho et al., 2012). The bacteria were restrictively attached to one-half side of the PEG microbeads, and the motility of the bacteriobot was clearly enhanced.

Generally, flagellar bacteria show vigorous random swimming motion at high speeds of 15–100 μm/s (Berg, 2003). The proposed bacteriobot, which acquires its motility from the bacteria, can also show random walk motion. The random walk motions of the bacteria can be changed into directional motions depending on the taxis of the bacteria (Eisenbach, 1996). Therefore, the taxis characteristics of bacteria are expected to change the random walk motions of a bacteriobot to directional motions. Among the various types of bacteria taxes, chemotaxis of bacteria has been actively studied for biomedical applications. Especially, *S. typhimurium* and *E. coli* can recognize their environments via their chemoreceptors (methyl-accepting chemotaxis proteins: MCPs) and show motility and directionality toward a chemo-attractant by flagella motor (Zhulin et al., 1997). In addition, the photo-taxes of *E. coli* and magneto-tactic bacterium (MTB) have been studied (Braatsch and Klug, 2004; Mokrani et al., 2010).

In this article, we adopt the *S. typhimurium* strain, which can be used as a diagnostic and a therapeutic biomedical tool (Min et al., 2008). By selective patterning of the bacteria on microbeads using BSA and using the submerging property of PS microbeads on agarose gel, a bacteriobot with enhanced motility was fabricated. The bacteriobot moved by the flagellar motion of *S. typhimurium*. The directional motility of the bacteriobot was controlled by the chemotaxis characteristics of the attached *S. typhimurium*. The chemotaxis of the bacteriobot using *S. marcescens* was reported, and the directional motility of the bacteriobot using *S. marcescens* was simply demonstrated (Kim et al., 2012; Traor´e et al., 2011). However, the directional motility of the bacteriobot using *S. marcescens* could not be statistically quantified. For the quantitative evaluation of the chemotactic directional motility of the bacteriobot, we proposed a microfluidic chamber which can generate a stable concentration gradient of chemotactic chemicals. In the concentration gradient of a chemo-attractant and chemo-repellent, the directional motilities of the bacteriobot were quantified and characterized.

Materials and Methods

Preparation of Bacteria

The strain of the bacteria used in this research was *S. typhimurium* ΔppGpp/*lux*/*gfp* (Min et al., 2008), which was genetically engineered through the defection of guanosine 5′-diphosphate-3′-diphosphate (ppGpp) to attenuate the toxicity and through the insertions of the Luciferase (*lux*) gene and the green fluorescent protein (*gfp*) gene to generate luminescence and fluorescence signals, respectively. The *S. typhimurium* should be cultured for 8 h on a mixture of Luria–Bertani (LB) agar plate (yeast: 0.5 g, tryptone: 1.0 g, NaCl: 1.0 g, agar: 1.0 g, de-ionized [DI] water: 100 mL), Ampicillin (Duchefa Biochemie, B.V., Haarlem, the Netherlands), and Kanamycin (Duchefa Biochemie) with a concentration of 50 μg/mL. Two milliliters of LB media (yeast: 0.5 g, tryptone: 1.0 g, NaCl: 1.0 g, DI water: 100 mL) was added into the culturing agar plate. The cultured bacteria were finally harvested using a cell scraper. The bacterial density of the final harvested bacteria solution was set to 2.5–3.0 optical density (OD)-600 using a spectrophotometer (UV mini-1240, Shimadzu Co. Kyoto, Japan). The high-density bacteria solution reduced the attachment time of the bacteria to the microstructure and increased the number of the attached bacteria on the microstructure.

Fabrication of Bacteriobot

For the fabrication of the bacteriobot, we used a rhodamin-labeled PS microbead (Polyscience, Warrington, PA) of 3 μm diameters. The rhodamin-labeled PS microbead can emit yellow-orange light (542 nm) upon 529 nm spectral line excitation. In addition, a PS microbead has a hydrophobic surface, on which bacteria can easily attach. For the enhancement of the motility of the bacteriobot, we selectively patterned the bacteria to the rhodamin-labeled PS microbead. Figure 1 shows the selective patterning procedure of the bacteria and the bacteria pattern result. Especially, Figure 1a shows the selective BSA (Sigma–Aldrich Chemical Co., St. Louis, MO) coating procedure based on the submerging property of the PS microbead on agarose gel, where BSA can hinder bacteria adhesion on the PS microbead. For selective BSA coating, agarose gel and PDMS (Sylgard 184 Silicone Elastomer Kit, Dow Corning, Midland, MI) were adopted. First, 1% agarose solution was prepared and poured into a petri dish. After the gelation of the agarose solution, a mixture solution of phosphate-buffered saline (PBS) and PS microbeads was spread onto the surface of the 1% agarose gel. After the PBS of the mixture solution was dried, the PS microbeads were positioned and submerged on the agarose gel surface. Second, a PDMS solution of Sylgard 184 A and Sylgard 184 B (Dow Corning) with a volume ratio of 10:1 was slowly poured onto the top of the agarose gel to submerge the PS microbeads. The PDMS solution on the agarose gel surface was cured at room temperature for 24 h. After curing, the PDMS substrate was detached from the agarose surface and the PS microbeads submerged in the agarose gel were transferred to the surface of the PDMS substrate. Third, after the washing procedure using DI water, the PS microbeads embedded in the PDMS substrate were soaked in 5% BSA solution for 3 h. Then, BSA was coated on one-half sides of the PS microbeads, and the

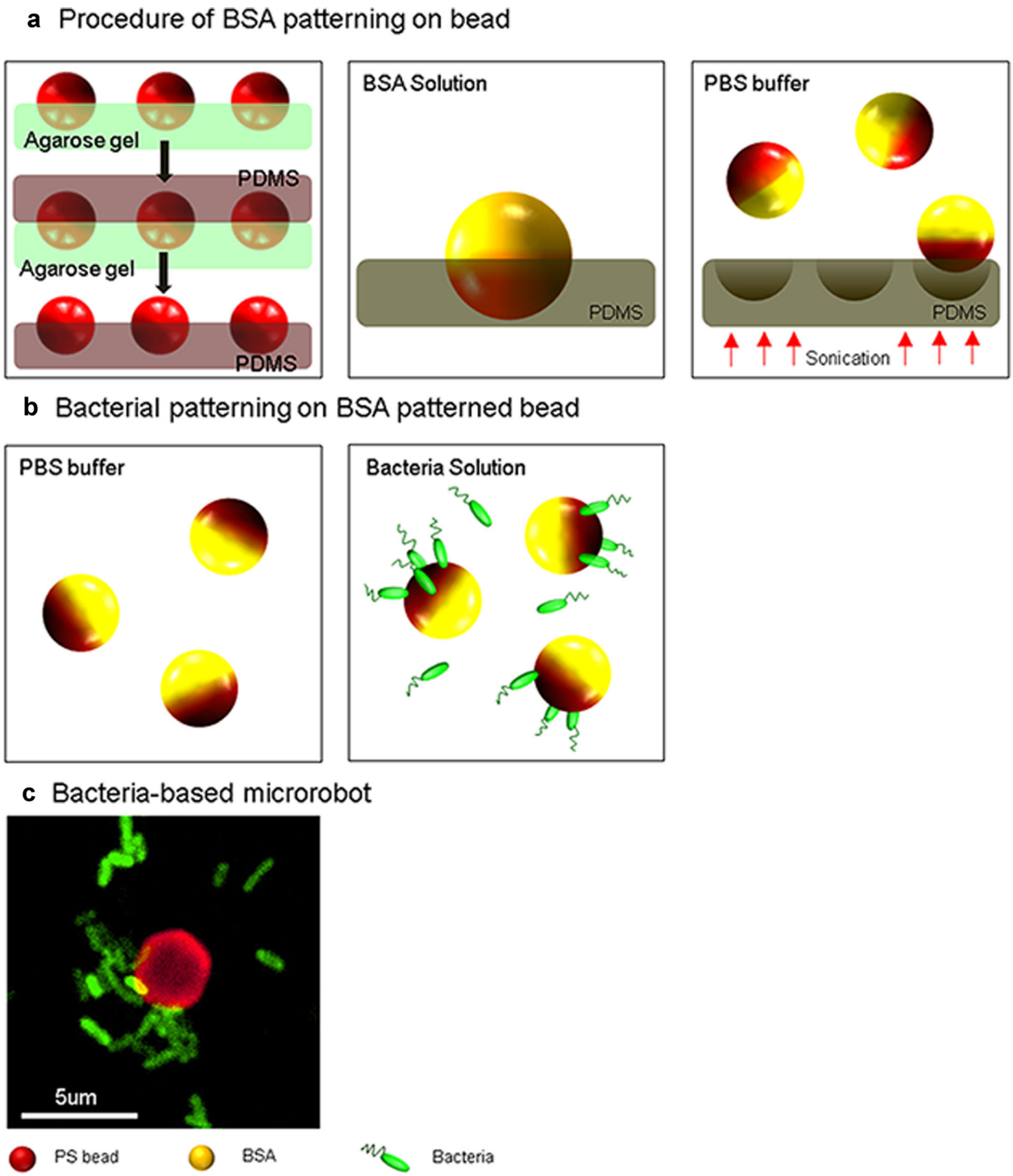

Figure 1. Fabrication procedure of bacteria-based microrobot (Bacteriobot): (**a**) procedure of BSA patterning on microbeads using the submerging property of PS microbeads on agarose gel, (**b**) selective bacterial patterning on PS microbeads, and (**c**) laser confocal scanning microscopic image of bacteriobot.

bacteria could be attached to the other half sides of the PS microbeads. The selective surface treated PS microbeads in the PDMS substrate were extracted by ultra-sonication. The extracted PS microbeads were then collected by centrifugation. Finally, by mixing the *S. typhimurium* strain and the selective BSA-coated PS microbeads in a motility buffer, the bacteria were attached onto the selectively BSA-coated surfaces of the PS microbeads. Figure 1b shows the procedure of bacterial patterning on the BSA patterned microbeads, and Figure 1c shows the confocal laser scanning microscope (TCS

SP5/AOBS/Tandem, Leica, Wetzlar, Germany) image of a fabricated bacteriobot. From Figure 1c, through the fabrication procedure of the bacteriobot, we found that the *gfp*-expressed fluorescent *S. typhimurium* (approx. 1–3 bacteria) were attached to a restricted region of the rhodamin-labeled PS microbead of 3 μm diameter.

Fabrication of Microfluidic Device for Chemotaxis Analysis

For the chemotaxis analysis of the bacteria and bacteriobot, a microfluidic device was designed and fabricated by conventional photo- and soft-lithography procedures. Figure 2a shows the web-type microfluidic chamber that was used for the motility analysis of the chemotactic bacteriobot under a chemical gradient. The web-type microfluidic chamber has vertical symmetry, consisting of arch-shaped and radial-formed micro-channels of 200 μm width. The left and right channels were connected with the center circle part of 2 mm diameter (Fig. 2b). In the photo-lithography procedure, first, a photo resistor (SU-8 2050, Microchem, Newton, MA) was coated on a 4 inch wafer using a spinner and soft-baked by a hot-plate. Next, the web-type microfluidic pattern was transferred onto the coated photo resistor by photo mask and ultraviolet (UV) exposures. After a post-exposure bake (PEB) and a developing step, an embossed web-type microfluidic pattern SU-8 mold was fabricated. The target height of the channel in the microfluidic device was set to 80 μm to allow the bacteria and bacteriobot to move freely in the channel. In the soft-lithography procedure, the embossed web-type pattern SU-8 mold became the master mold and replicas of the microfluidic device were produced. PDMS solution was slowly poured on the top of the SU-8 mold, where the PDMS solution is a mixture of PDMS solution of Sylgard 184 A and Sylgard 184 B at a volume ratio of 10:1. After the curing the PDMS solution in a dry oven, the PDMS replica was detached from the SU-8 mold and an intaglio web-type microfluidic patterned PDMS was obtained. After punching to form the inlet and outlet of the microfluidic device, the PDMS was bonded with glass by using an O_2 plasma asher and a dry oven. Finally, we fabricated a web-type microfluidic chamber for the evaluation of the bacteria's and bacteriobot's chemotaxis shown in Figure 2c.

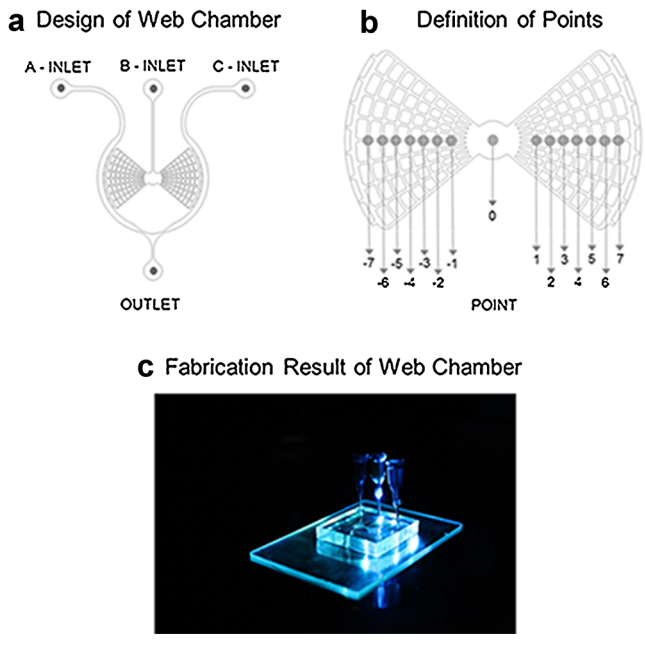

Figure 2. Development of microfluidic chamber for evaluation of bacteria and bacteriobot chemotaxis: (**a**) design of microfluidic chamber, (**b**) definition of point in microfluidic chamber, and (**c**) fabrication result of developed microfluidic chamber.

Experimental Setup

The web-type microfluidic chamber consists of three inlets at the upper side and one outlet at the lower side (Fig. S1a). The left inlet (A-INLET) is for the PBS buffer, the right inlet (C-INLET) is for chemo-effectors (chemo-attractant or chemo-repellent), and the central inlet (B-INLET) is for the bacteria or bacteriobot solution injection. We adopted 20 mM L-aspartic acid (Sigma–Aldrich Chemical Co.) as the chemo-attractant and 40 mM $NiSO_4$ (Sigma–Aldrich Chemical Co.) as the chemo-repellent (Barak and Eisenbach, 1999; Kim and Breuer, 2007). For the quantitative evaluation, the points of region of interest (ROI; $100 \times 100\ \mu m^2$) were defined from −6 to 6 in Figure 2b. First, the PBS buffer (A- and B-INLET) and the chemo-effectors (chemo-attractant or chemo-repellent) containing buffer (C-INLET) were loaded into the INLET reservoirs using a 19-gauge plastic needle. When the buffers flowed out to OUTLET, the OUTLET reservoir was closed with a blocked 19-gauge plastic needle. After 10 min, the PBS buffer was replaced by the same volume of the highly concentrated bacteria or bacteriobot solution at the B-INLET. After 20 min, the distribution of bacteria or bacteriobot in the web-type chamber was measured by a fluorescence microscope (Nikon T*i*-U microscope; Nikon USA, Melville, NY; Fig. S1).

Analysis of Bacteria and Bacteriobot Distribution

For the measurement of the bacteria or bacteriobot distribution in the microfluidic chamber, we used a fluorescence microscope (Nikon T*i*-U microscope) and a wide-range excitation UV filter (T*i*-FL Epi-Fl Filter Turret, Nikon Inc.). The images captured by the fluorescence microscope were converted into JPEG files using the NIS-Element BR 3.1 program (Nikon USA). Images of *gfp*-expressed *S. typhimurium* at every point in the microfluidic chamber were obtained using the FITC filter. Because it is very difficult to count the bacteria directly from the images, we indirectly estimated the bacterial cell number by comparing the measured fluorescence intensity, the bacteria OD-600 value, and

viable cell count. In addition, the fluorescence intensity of *gfp*-expressed *S. typhimurium* was obtained using the conventional Image J program.

For the distribution analysis of the bacteriobots, a fluorescent image of the bacteriobots was captured using a rhodamine filter because the bacteriobots were fabricated using rhodamin-labeled PS microbeads. The distribution of the bacteriobots was measured by counting the bacteriobots directly. The quantitative distribution of the bacteria or the bacteriobot was calculated by the following formula:

$$P_i = \frac{N_i}{\sum_{i=-6}^{6} N_i} \times 100 \quad (1)$$

where P_i denotes the distribution percentage of objects and N_i means the detected number of objects (bacteria or bacteriobot) at ith point in ROI.

Statistics

The above quantification analysis data were presented as mean values with a standard deviation, and statistical significance was determined using the ANOVA test (StatView; Abacus Concepts Inc., Berkeley, CA). All experiments were performed at least three times on separate days, and the data presented herein are the representative results from all repetitions.

Results

Chemical Concentration Gradient in Microfluidic Chamber

For the visual verification of the concentration gradients, we adopted a mixed solution of motility buffer and trypan-blue stain (GIBCO BRL, Gaithersburg, MD) instead of a chemo-repellent or a chemo-attractant. Figure S2a shows the chemical concentration gradient between deionized (DI) water in the center and trypan-blue stain mixed solution in the outer channel. Figure S2b shows the OD values at every point, where an OD value means the concentration of the blue dye solution. Similarly, by monitoring the chemical concentration gradient using a red dye in the microfluidic chamber, we found that the concentration gradient of the red dye was established 10 min after the injection of the chemicals and was maintained for over 80 min in the web chamber, which was enough time for the measurement of the bacteria and bacteriobot chemotaxis (Fig. S3). From the results, it was confirmed that the developed microfluidic chambers could generate a continuously stable chemical concentration gradient of chemo-effectors and could be used for the chemotaxis test of the bacteria and bacteriobot.

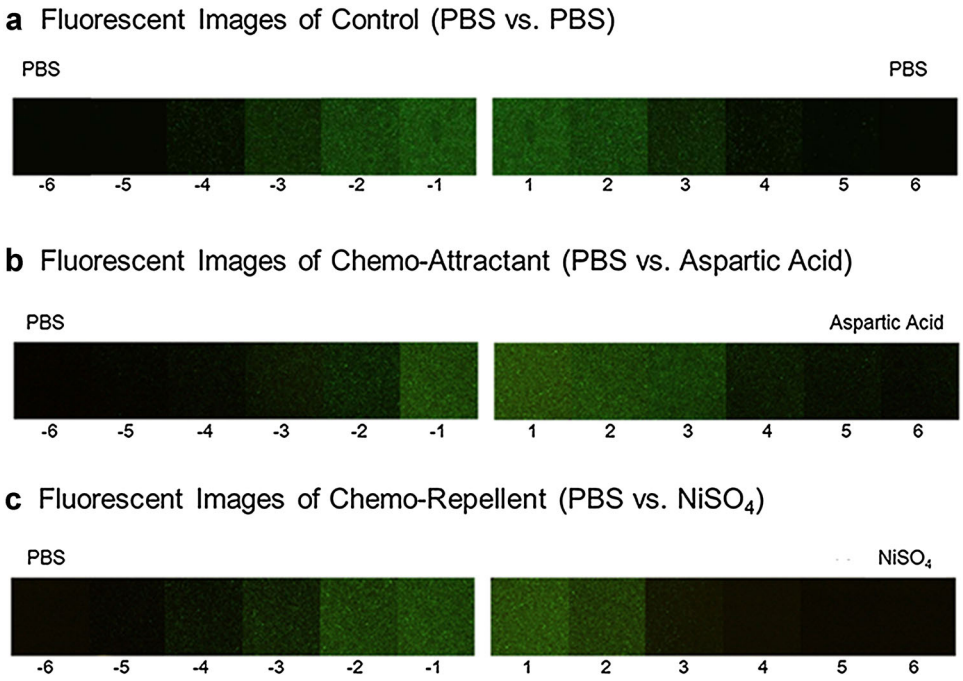

Figure 3. Fluorescent microscopic images of bacteria distribution at each point in microfluidic chamber: (**a**) control case (PBS vs. PBS), (**b**) chemo-attractant case (PBS vs. L-aspartic acid), and (**c**) chemo-repellent case (PBS vs. $NiSO_4$). When the gradients of the chemo-effectors were generated in the web-type chamber, the concentrated bacteria solution was loaded into the middle of the chamber. After 20 min, the distribution of the bacteria in the web-type chamber was measured by a fluorescence microscope. The experiments were conducted several times (three or more times) on separate days. Reproducible results were obtained and representative data are shown in the figures.

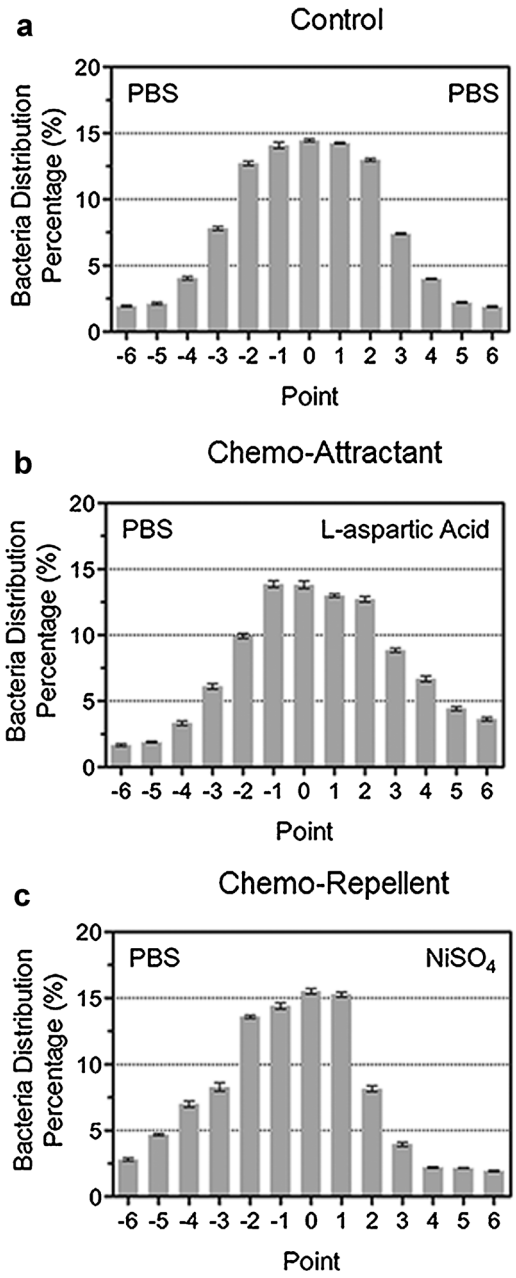

Figure 4. Percentage of bacteria distribution at each point in microfluidic chamber: (**a**) control case (PBS vs. PBS), (b) chemo-attractant case (PBS vs. 20 mM L-aspartic acid), and (**c**) chemo-repellent case (PBS vs. 40 mM $NiSO_4$). The experiments were conducted several times (three or more times) on separate days. Reproducible results were obtained and representative data are shown in the figures.

Chemotactic Behavior of Bacteria

For the chemotaxis tests of *S. typhimurium*, the following three tests were carried out. First, for the control experiment, PBS buffer solution was simultaneously injected into the A-INLET and the C-INLET. Second, for the chemo-attractant experiment, 20 mM L-aspartic acid (chemo-attractant) was injected into the C-INLET and PBS buffer was injected into the A-INLET. Finally, for the chemo-repellent experiment, 40 mM $NiSO_4$ (chemo-repellent) was injected into the C-INLET and PBS buffer was injected in the A-INLET (Fig. S1). Figure 3 shows the resultant fluorescent images of the three chemotaxis tests at every point in the microfluidic chamber. Because the *S. typhimurium* ΔppGpp/*lux*/*gfp* expresses green fluorescence, the bright-green region means a high density of bacteria, and the dark region means a low density of bacteria. In the control experiment, when *S. typhimurium* were injected in the B-INLET of the microfluidic chamber, the bacteria would equally spread out in all directions along the channel in the chamber (Fig. 3a). Figure 3b depicts the chemo-attraction result of *S. typhimurium* in the microfluidic chamber, where the high density of the *S. typhimurium* moved toward the chemo-attractant direction. Finally, Figure 3c shows the resultant images of the chemo-repellent effect. In Figure 3c, *S. typhimurium* show less motility toward the chemo-repellent direction than toward the PBS-control direction.

For the evaluation of the chemotaxis of *S. typhimurium*, the images of Figure 3 were converted to give the number of *S. typhimurium* by using the bacteria fluorescence intensity and the Image J program. By using this relation and the distribution percentage of Equation (1), the above experimental fluorescent images are summarized in Figure 4a–c, which directly shows the distribution of *S. typhimurium*. Figure 4a is the result of the control experiment; it shows the symmetric distribution of *S. typhimurium* from points −6 to 6. However, Figure 4b depicts the increment of *S. typhimurium* distribution at the chemo-attractant (L-aspartic acid) region and Figure 4c shows the decrement of the bacteria distribution at the chemo-repellent ($NiSO_4$) region. Consequently, through the developed microfluidic chamber and the image processing, the chemotactic behavior of the bacteria was demonstrated and evaluated.

For a more detailed analysis of the chemotaxis performance of *S. typhimurium*, the differences of the *S. typhimurium* distribution between the chemotaxis and the control results were measured. Based on the distribution of *S. typhimurium* in the Figure 4a control experiment, the increments or decrements in the distribution of *S. typhimurium* in Figure 4b (chemo-attractant) and Figure 4c (chemo-repellent) were calculated and plotted in Figure 5. Figure 5a shows the difference in the bacterial distribution percentage between the chemo-attractant test and the control. Through this comparison, we found that the distribution of *S. typhimurium* from points 3 to 6 in the chemo-attractant region had considerably increased by about 16%. Similarly, Figure 5b shows the difference in the bacterial distribution percentage between the chemo-repellent test and the control. There was a big decrease of *S. typhimurium* distribution from points 2 to 4 in the chemo-repellent region by about 22%.

Chemotactic Behavior of Bacteriobot

Similarly, for the chemotaxis tests of the bacteriobot, the images of ROI at every point from left (−6) to right (6) were taken (Fig. 6). First, in the control case, PBS instead of the

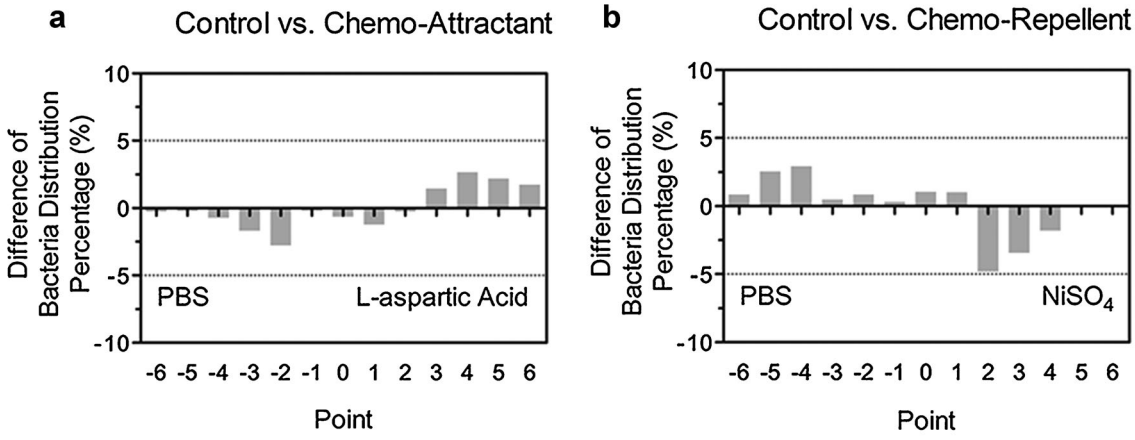

Figure 5. Difference of bacteria distribution percentage: (**a**) chemo-attractant (20 mM L-aspartic acid) versus Control and (**b**) chemo-repellent (40 mM $NiSO_4$) versus Control. All experiments were conducted three or more times on separate days. Reproducible results were obtained and representative data are shown in the figures.

chemo-effector was injected into the A-INLET and the C-INLET. When the bacteriobots were injected into B-INLET, the bacteriobots moved symmetrically from points −4 to 4, but the directional motility of the bacteriobots was not observed (Fig. 6a). Second, when the bacterial chemo-attractant, 20 mM L-aspartic acid, was injected into the right side inlet (C-INLET), the distribution of the bacteriobots in the right side of the microfluidic chamber was significantly increased toward the chemo-attractant (Fig. 6b). Finally, we injected the bacterial chemo-repellent, 40 mM $NiSO_4$, into the right inlet (C-INLET) and generated a chemical gradient of the chemo-repellent. In the chemo-repellent case, the distribution of the bacteriobots in the right side of the microfluidic device was significantly decreased in resistance to the chemo-repellent, and the distribution of the bacteriobots on the left side was increased (Fig. 6c).

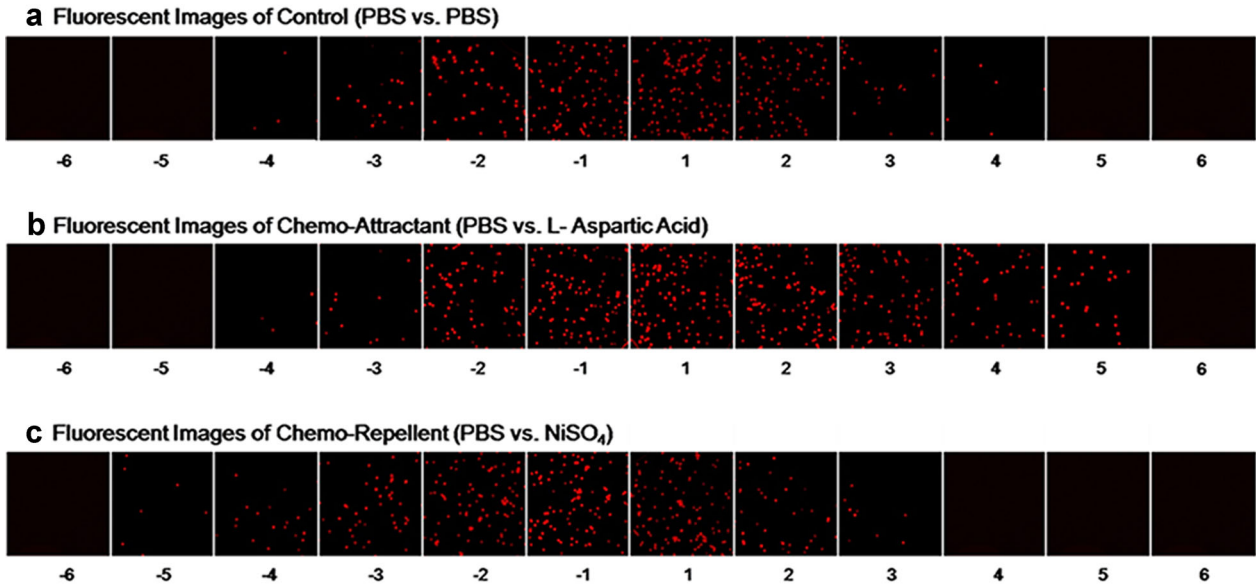

Figure 6. Fluorescent microscopic images of bacteriobot distribution at each point in microfluidic chamber: (**a**) Control case (PBS vs. PBS), (**b**) Chemo-attractant case (PBS vs. L-aspartic acid), and (**c**) Chemo-repellent case (PBS vs. $NiSO_4$). When the gradients of the chemo-effectors were generated in the web-type chamber, the concentrated bacteriobot solution was loaded into the middle of the chamber. After 20 min, the distribution of the bacteriobot in the web-type chamber was measured by a fluorescence microscope. The experiments were conducted several times (three or more times) on separate days. Reproducible results were obtained and representative data are shown in the figures.

Consequently, like the bacteria, the bacteriobots showed positive chemotaxis toward the chemo-attractant gradient and negative chemotaxis against the chemo-repellent.

In order to quantify the distribution of the bacteriobots to the chemo-effectors, we directly counted the number of bacteriobots at every point in Figure 6 and then the number of bacteriobots at every point was converted into a distribution percentage of the bacteriobots through Equation (1). Figure 7a shows a symmetric normal Gaussian distribution of the bacteriobots in the control case. Most of the bacteriobots (over 80%) were positioned in the section from points −2 to 2. Figure 7b shows the positive chemotactic motility of the bacteriobots toward the 20 mM L-aspartic acid. The bacteriobots appeared up to 5 point, and the distribution of the bacteriobots in the right part of the microfluidic chamber was significantly increased. On the other hand, Figure 7c shows the negative chemotactic motility of the bacteriobot against the 40 mM $NiSO_4$. Figure 8a shows the difference in the bacteriobot distribution percentage between the chemo-attractant test and the control. Through this comparison, we found that the distribution of bacteriobots from points 3 to 5 in the chemo-attractant region had considerably increased by about 14%. Similarly, Figure 8b shows the difference in the bacteriobot distribution percentage between the chemo-repellent test and the control. There was a big decrease of *S. typhimurium* distribution from points 1 to 3 in the chemo-repellent region by about 13%.

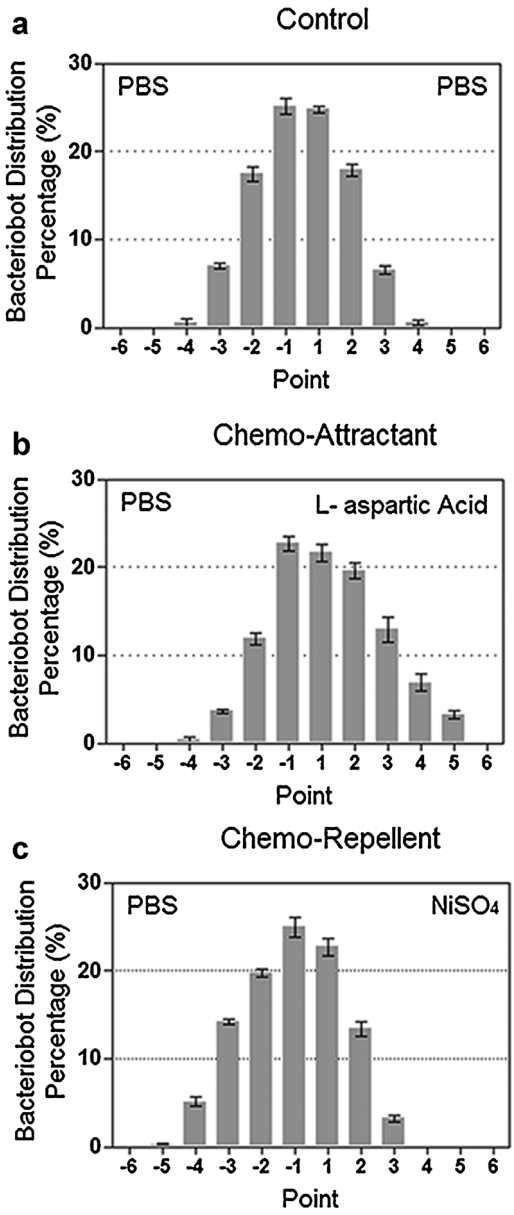

Figure 7. Percentage of bacteriobot distribution at each point in microfluidic chamber: (**a**) Control case (PBS vs. PBS), (**b**) chemo-attractant case (PBS vs. 20 mM L-aspartic acid), and (**c**) chemo-repellent case (PBS vs. 40 mM $NiSO_4$). The experiments were conducted several times (three or more times) on separate days. Reproducible results were obtained and representative data are shown in the figures.

Discussion

Microrobots can be used in various applications, such as the biological, medical, environmental, space, and military applications (Requicha, 2003; Sharma and Mittal, 2008). Nevertheless, microrobot development still faces many challenges, such as the fabrication of micro-sized actuators and sensors (Sitti, 2009). To overcome these challenges, we investigated bacteria-based microrobots (Bacteriobot) actuated by flagellar bacteria such as *S. marcescens* and *S. typhimurium* (Cho et al., 2012; Park et al., 2010). Flagellar bacteria offer various advantages as a microactuation and microsensing for flagellar-based motors and receptor response displays. They can be controlled by various taxis methods such as light, magnetic field, and chemical gradients (Darnton et al., 2004; Sowa and Berry, 2008).

In the development of the bacteriobot, it was found that bacterial patterning on PS microbead surfaces had an important effect on the enhancement of bacteriobot's motility and directionality. When one side of the PS microbead was exposed by RIE plasma, the bacteria would attach only on the other side of the PS microbead surface because of hydrophobicity. The bacteria-actuated microrobot made by RIE plasma exposure showed approximately two times higher average velocities than a PS microbead attached with bacteria by a normal method ($V = 28.2 \pm 10.5$ μm/s vs. $V = 14.8 \pm 1.1$ μm/s) (Behkam and Sitti, 2008). However, these patterning techniques have some limitations that is difficult to modify the surface of the microstructure using various proteins such as BSA, poly-L-lysine (PLL), collagen, or antibodies (Cho et al., 2012; Park et al., 2010).

For evaluation of bacteria chemotaxis, it is necessary to focus on the flow effect of the test bed and the concentration gradient of a specific substance. However, it is difficult to maintain a uniform concentration gradient of chemo-effectors without flow in the test bed. Therefore, it would be very effective and useful to develop a bacteria chemotaxis evaluation method that could have a stable concentration gradient of chemo-effectors without flow in the test bed. For

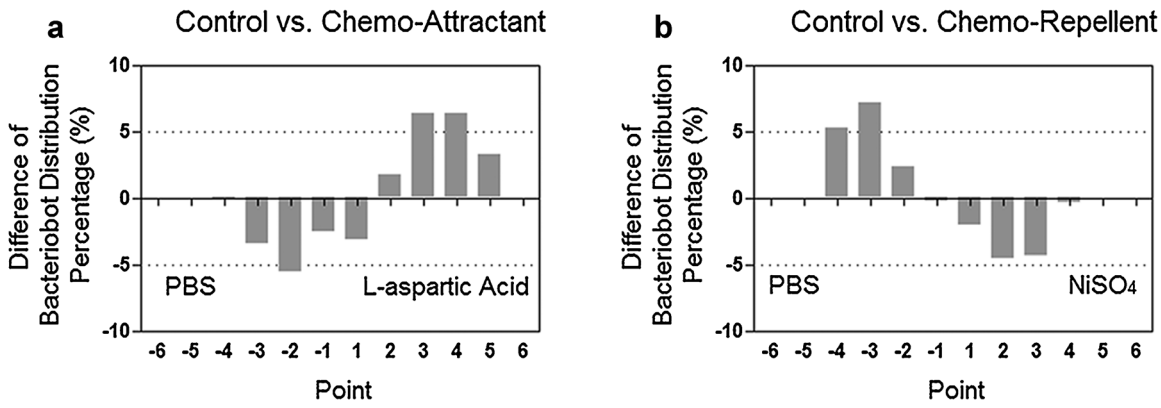

Figure 8. Difference of bacteriobot distribution percentage: (**a**) chemo-attractant (20 mM L-aspartic acid) versus control, and (**b**) chemo-repellent (40 mM $NiSO_4$) versus control. All experiments were conducted three or more times on separate days. Reproducible results were obtained and representative data are shown in the figures.

the evaluation of the bacterial chemotaxis, an agar plate assay and a capillary assay were used (Ahmed and Stocher, 2008; Bainer et al., 2003; Wolf and Berg, 1989). The agar plate assay is used to investigate the direction of bacterial proliferation on a semisolid agar medium. It is a very simple and convenient method (Wolf and Berg, 1989), but it cannot measure the motility of bacteria in a liquid medium. The capillary assay is used to investigate the movement of bacteria in a liquid medium when the chemo-attractant or chemo-repellent chemicals are minutely released from a capillary tube. The capillary assay is also a very simple and powerful method with some benefits for the chemotaxis evaluation of high-motility flagellar bacteria (Bainer et al., 2003). However, because of the possible diffusion of chemotaxis chemicals in a liquid medium in a very short time period, it is very difficult to measure and 80 fy the chemotaxis phenomena of low-motility bacteria. In order to overcome the above-mentioned problems of the chemotaxis assays, many researchers have proposed bacterial chemotaxis evaluation methods that use microfluidics, which guarantee free movements of the bacteria in a liquid medium, generate the concentration gradient of chemotaxis chemicals, and measure the motility of bacteria (Englert et al., 2009; Jeon et al., 2009; Lanning et al., 2008; Mao et al., 2003; Stocker et al., 2008). However, it is very difficult to generate uniform concentration gradients and directly measure bacterial motility itself because of flow disturbances. In addition, the chemotaxis of low-motility bacteria is also very difficult to evaluate because of the microchannel flow. On the other hand, there are unsteady gradient-evaluation methods without flow in the micro-channel, where bacteria can move freely in the medium of the microchannel (Cheng et al., 2007; Seymour et al., 2009). However, the sustainable chemical-gradient period is short, so it is not easy to evaluate the chemotaxis of low-motility bacteria. Finally, there are steady gradient-evaluation methods without flow in a microchannel that can allow free movement of bacteria in the medium and sustain the chemical gradient for a long period of time (Ahmed et al., 2010; Diao et al., 2006; Wu et al., 2006). However, these evaluation methods are very complex and they require expensive procedures and devices. Also, hydro-gels with low-diffusion velocity can be used for maintaining a uniform concentration gradient, but they may interrupt bacterial movement.

For this reason, we proposed a bacteriobot constructed by the combination of flagellar *S. typhimurium* and a selective BSA-patterned PS microbead using the submerging property of the PS microbead on agarose gel (Fig. 1). In addition, for the evaluation of the chemotactic behavior of the bacteria and bacteriobots, we developed a web-type chamber microfluidic platform that can maintain a continuous chemical concentration gradient and remove the flow effect in the microfluidic chamber (Fig. 2).

Firstly, we verified the chemotaxis characteristics of the bacteria and bacteriobot using chemo-effectors (20 mM L-aspartic acid as the chemo-attractant and 40 mM $NiSO_4$ as the chemo-repellent) in the microfluidic chamber (Figs. 3–8). Similar with the chemotactic bacteria, the bacteriobot showed positive and negative chemotaxis motilities to the chemo-attractant and the chemo-repellent, respectively. The chemotactic directional motility of the bacteriobot was determined by the intrinsic characteristics of the bacteria. Therefore, the bacteriobot showed chemotactic motility similar to that of the attached bacteria.

Especially, we adopted the bacterial strain *S. typhimurium*, which has been used for tumor targeting and therapy (Min et al., 2008; Zhao et al., 2005). The bacteria have properties such as tumor recognition and directional motility that will be important for new biomedical applications. The bacteria can be guided by a chemical gradient and can arrive at the source of the chemo-attractant. Through the integration of the tumor targeting bacteria and anti-cancer medicine (drug and therapeutic bacteria), we expect an advanced novel concept of a biomedical microrobot for active drug delivery.

Conclusions

A bacteriobot is actuated by the flagellar motion of bacteria and can carry out sensing functions by the chemotaxis of the

bacteria. In this study, we suggested the fabrication of a bacteriobot using the combination of flagellar *S. typhimurium* bacteria and a selectively BSA patterned PS microbead. The motility of the bacteriobot was enhanced by the selective bacterial patterning. The directional motility was analyzed quantitatively by using chemo-effectors, L-aspartic acid (chemo-attractant) and $NiSO_4$ (chemo-repellent), in a microfluidic device that could generate a continuously stable chemical gradient. The chemotactic properties of the bacteria were quantified by image processing of fluorescent images. In the concentration gradients of the chemo-attractant and chemo-repellent, the ratios of the distribution percentages of the bacteria were increased by 16% and decreased by 22%, respectively. In addition, the directional motilities of the bacteriobot were increased by14% in the chemo-attractant gradient and decreased by 13% in the chemo-repellent gradient, respectively. Based on these results, we will develop a bacteriobot with various useful properties such as high motility and effective tumor targeting, and anti-tumor effects containing drug delivery systems. In the future, we can expect a bacteriobot with a tumor targeting bacteria for use as a biomedical microrobot for tumor diagnosis and therapy.

References

Ahmed T, Stocher R. 2008. Experimental verification of the behavioral foundation of bacterial transport parameters using microfluidics. Biophys J 95:4481–4493.

Ahmed T, Shimizu TS, Stocker R. 2010. Bacterial chemotaxis in linear and nonlinear steady microfluidic gradients. Nano Lett 10:3379–3385.

Bainer R, Park H, Cluzel P. 2003. A high-throughput capillary assay for bacterial chemotaxis. J Microbiol Meth 55:315–319.

Barak RB, Eisenbach M. 1999. Chemotactic-like response of *Escherichia coli* cell slacking the known chemotaxis machinery but containing overexpressed CheY. Mol Microbiol 31:1125–1137.

Behkam B, Sitti M. 2008. Effect of quantity and configuration of attached bacteria on bacterial propulsion of microbeads. Appl Phys Lett 93:223901–223903.

Berg HC. 2003. The Rotary motor of bacterial flagella. Annu Rev Biochem 72:19–54.

Braatsch S, Klug S. 2004. Blue light perception in bacteria. Photosynth Res 79:45–57.

Bren A, Eisenbach M. 2000. How signals are heard during bacterial chemotaxis: Protein–protein interactions in sensory signal propagation. J Bacteriol 182:6865–6873.

Cheng SY, Heilman S, Wasserman M, Archer S, Shuler ML, Wu MM. 2007. A hydrogel-based microfluidic device for the studies of directed cell migration. Lab Chip 7:763–769.

Cho SH, Park SJ, Ko SY, Park JO, Park SH. 2012. Development of bacteria-based microrobot using biocompatible poly(ethylene glycol). Biomed Microdevices 14:1019–1025.

Darnton N, Turner L, Breuer K, Berg HC. 2004. Moving fluid with bacterial carpets. Biophys J 86:1863–1870.

Diao JP, Young L, Kim S, Fogarty EA, Heilman SM, Zhou P, Shuler ML, Wu MM, DeLisa MP. 2006. A three-channel microfluidic device for generating static linear gradients and its application to the quantitative analysis of bacterial chemotaxis. Lab Chip 6:381–388.

Eisenbach M. 1996. Microreview control of bacterial chemotaxis. Mol Microbiol 20:903–910.

McEldowney S, Fletcher M. 1986. Variability of the influence of physicochemical factors affecting bacterial adhesion to polystyrene substrata. Appl Environ Microbiol 52:460–465.

Englert DL, Manson MD, Jayaraman A. 2009. Flow-based microfluidic device for quantifying bacterial chemotaxis in stable, competing gradients. Appl Environ Microbiol 75:4557–4564.

Jeon H, Lee Y, Jin S, Koo S, Lee CS, Yoo JY. 2009. Quantitative analysis of single bacterial chemotaxis using a linear concentration gradient microchannel. Biomed Microdevices 11:1135–1143.

Kasinskas RW, Forbes NS. 2006. *Salmonella typhimurium* specifically chemotaxis and proliferate in heterogeneous tumor tissue in vitro. Biotechnol Bioeng 94:710–721.

Kim MJ, Breuer KS. 2007. Controlled mixing in microfluidic systems using bacterial chemotaxis. Anal Chem 79:955–959.

Kim D, Liu A, Diller E, Sitti M. 2012. Chemotactic steering of bacteria propelled microbeads. Biomed Microdevices 14:1009–1017.

Lanning LM, Ford RM, Long T. 2008. Bacterial chemotaxis transverse to axial flow in a microfluidic channel. Biotechnol Bioeng 100:653–663.

Leschner S, Westphal K, Dietrich N, Viegas N, Jablonska J, Lyszkiewicz M, Lienenklaus S, Falk W, Gekara N, Loessner H, Weiss S. 2009. Tumor invasion of *Salmonella enterica* serovar Typhimurium is accompanied by strong hemorrhage promoted by TNF-alpha. PLoS ONE 4:e6692.

Mao H, Cremer PS, Manson MD. 2003. A sensitive, versatile microfluidic assay for bacterial chemotaxis. Proc Natl Acad Sci USA 100:5449–5454.

Min JJ, Nguyen VH, Kim HJ, Hong T, Choy HE. 2008. Quantitative bioluminescence imaging of tumor-targeting bacteria in living animals. Nat Protoc 3:1–8.

Mokrani N, Felfoul O, Zarreh FA, Mohammadi M, Aloyz R, Batist G, Martel S. 2010. Magnetotactic bacteria penetration into multicellular tumor spheroids for targeted therapy. IEEE Eng Med Biol Soc (EMBC) 2010:4371–4374.

Park SJ, Bae HI, Kim JH, Lim BJ, Park JO, Park SH. 2010. Motility enhancement of bacteria actuated microstructures using selective bacteria adhesion. Lab Chip 10:1706–1711.

Requicha AAG. 2003. Nanorobots, NEMS, and nanoassembly. IEEE Nanoelecton Nanoprocess 91:1922–1933.

Seymour JR, Ahmed T, Durham WM, Stocker R. 2009. Resource patch formation and exploitation throughout the marine microbial food web. Am Nat 173:E15–E29.

Sharma NN, Mittal RK. 2008. Nanorobot movement: Challenges and biologically inspired solutions. Int J Smart Sens Intell Syst 1:87–108.

Sitti M. 2009. Miniature devices: Voyage of the microrobots. Nature 458: 1121–1122.

Sowa Y, Berry RM. 2008. Bacterial flagellar motor Q Rev Biophys 41:103–132.

Stocker R, Seymour JR, Samadani A, Hunt DE, Polz MF. 2008. Rapid chemotactic response enables marine bacteria to exploit ephemeral microscale nutrient patches. Proc Natl Acad Sci USA 105:4209–4214.

Traor´e MA, Sahari A, Behkam B. 2011. Computational and experimental study of chemotaxis of an ensemble of bacteria attached to a microbead. Phys Rev E Stat Nonlin Soft Matter Phys 84:061908-1–061908-6.

Wadhams CH, Armitage JP. 2004. Making sense of it all: Bacterial chemotaxis. Nature 5:1024–1037.

Wolf AJ, Berg HC. 1989. Migration of bacteria in semisolid agar. Proc Natl Acad Sci USA 86:6973–6977.

Wu HK, Huang B, Zare RN. 2006. Generation of complex, static solution gradients in microfluidic channels. J Am Chem Soc 128:4194–4195.

Yoo JW, Irvine DJ, Discher DE, Mitragotri S. 2011. Bio-inspired, bioengineered and biomimetic drug delivery carriers. Nat Rev Drug Discov 10:521–535.

Zhao M, Yang M, Li XM, Jiang P, Baranov E, Li S, Xu M, Penman S, Hoffman RM. 2005. Tumor-targeting bacterial therapy with amino acid auxotrophs of GFP-expressing *Salmonella typhimurium*. Proc Natl Acad Sci USA 3:755–760.

Zhulin IB, Rowsell EH, Johnson MS, Taylor BL. 1997. Glycerol elicits energy taxis of *Escherichia coli* and *Salmonella typhimurium*. J Bacteriol 179:3196–3201.

Supporting Information

Additional supporting information may be found in the online version of this article at the publisher's website.